Acta Oceanol. Sin., 2018, Vol. 37, No. 3, P. 1–7
DOI: 10.1007/s13131-018-1195-3
http://www.hyxb.org.cn
E-mail: hyxbe@263.net

The winter western boundary current of the South China Sea: physical structure and volume transport in December 1998

LI Li[1]*, GUO Xiaogang[1], WU Risheng[1]

[1] Third Institute of Oceanography, State Oceanic Administration, Xiamen 361005, China

Received 20 October 2017; accepted 20 November 2017

Abstract

The unique survey in December 1998 mapped the entire western boundary area of the South China Sea (SCS), which reveals the three-dimensional structure and huge volume transport of the swift and narrow winter western boundary current of the SCS (SCSwwbc) in full scale. The current is found to flow all the way from the shelf edge off Hong Kong to the Sunda Shelf with a width around 100 km and a vertical scale of about 400 m. It appears to be the strongest off the Indo-China Peninsula, where its volume transport reached over 20×10^6 m^3/s. The current is weaker upstream in the northern SCS to the west of Hong Kong. A Kuroshio loop or detached eddy intruded through the Luzon Strait is observed farther east where the SCSwwbc no more exists. The results suggest that during the survey the SCSwwbc was fed primarily by the interior recirculation of the SCS rather than by the "branching" of the Kuroshio from the Luzon Strait as indicated by surface drifters, which is likely a near-surface phenomenon and only contributes a minor part to the total transport of the SCSwwbc. Several topics related to the SCSwwbc are also discussed.

Key words: South China Sea, western boundary current, winter, hydrographic structure, volume transport

Citation: Li Li, Guo Xiaogang, Wu Risheng. 2018. The winter western boundary current of the South China Sea: physical structure and volume transport in December 1998. Acta Oceanologica Sinica, 37(3): 1–7, doi: 10.1007/s13131-018-1195-3

1 Introduction

It has long been known that the monsoon-driven surface circulation in the South China Sea (SCS) is strongly intensified near its western boundary, where the current seasonally reverses and appears much stronger in winter when the surface current off the Indo-China Peninsula (ICP) often exceeds 100 cm/s (Wyrtki, 1961). In the northeast monsoon season, this swift western boundary current flows southwestward over the continental slope of the northern SCS and turns southward streaming along the ICP coast, appearing as the most distinct feature of the basin-wide circulation (Li, 2008; Fang et al., 2012). Even so, this strong current has rarely been investigated systematically until recently (Fang et al., 2012; Wang et al., 2013).

Today, this strong winter current has caught the attention of researchers, and has been widely investigated based on observations from satellite altimetry (Li et al., 2000; Lyu et al., 2016; Quan et al., 2016; Zhang et al., 2016) and from satellite-tracked surface drifting buoys (Li et al., 2000; Centurioni et al., 2004, 2009; He and Wang, 2009; Zhang et al., 2016), based on model outputs and reanalysis data in public domains (Tian et al., 2015; Quan et al., 2016), and based on numerical modeling (Dong et al., 2013). The results of these investigations generally supported the finding of Wyrtki (1961), and further revealed several new aspects of the winter western boundary current of the SCS (SCSwwbc). They showed, for example, that the current is quite variable on both interannual and intraseasonal time scales, and it interacts strongly with mesoscale eddies propagated from the interior of the SCS. One may refer to Fang et al. (2012) and Wang et al. (2013) for their valuable reviews about these recent advances.

In spite of these progresses, our knowledge about the SCSwwbc is still very much confined to two-dimensional observations on the surface and model results. No observation at depth is available in the literature so far, which addresses the three-dimensional (3-D) structure of the SCSwwbc in full length scale, although that is the most important.

In this paper, we re-examine our observational results from a historical cruise conducted in December 1998, led by the Third Institute of Oceanography (Wu et al., 2002), which was a unique synoptic survey that mapped the entire western boundary area of the SCS from the Luzon Strait (LS) to the Sunda Shelf in deep winter. We intend to present a full image about the 3-D structure and volume transport of the SCSwwbc by using direct observations.

2 Observations

The field survey, which lasted from the end of November 1998 to the New Year's Eve (Wu et al., 2002), included nine transects across the western and northern boundary areas of the SCS (Table 1); most of them were perpendicular to the shorelines roughly (Fig. 1). Underway acoustic Doppler current profiler (ADCP) measurements were conducted using an RDI-VM150. Data at hydrographic stations were taken using a Neil Brown Mark III conductivity/temperature/depth profiler (CTD).

All data were quality controlled to discard bad data before our analysis. Since the amplitude of the barotropic tidal current off the slope of the northern SCS (Zu et al., 2008) is generally one or-

Foundation item: The National Basic Research Program (973 Program) of China under contract Nos 2009CB421205 and 2011CB40350; the National Key Research and Development Program of China under contract No. 2016YFC1402607; the State Oceanic Administration Special Grant of China under contract No. HY126-04-02-03.
*Corresponding author, E-mail: lili@tio.org.cn

Table 1. Observational information

Section ID	Date	Observation		Section coverage	
		CTD	Along-track ADCP	Start	End
A	1998.12.07	S043–S048	yes	8.5°N, 109.0°E	6.3°N, 113.5°E
	1998.12.14	S039–S041	yes		
B	1998.12.14–15	no	yes	8.5°N, 108.8°E	8.7°N, 112.0°E
C	1998.12.15–17	S030–S035	yes	11.0°N, 109.6°E	9.5°N, 113.0°E
D	1998.12.19–21	S024–S027	yes	11.0°N, 109.5°E	12.0°N, 112.0°E
E	1998.12.26	S016–S020	yes	15.5°N, 110.0°E	15.0°N, 113.0°E
F	1998.12.21–23	no	yes	14.0°N, 109.5°E	18.2°N, 112.0°E
G	1998.12.27	S001–S008	yes	21.0°N, 111.0°E	17.5°N, 114.5°E
H	1998.11.28	S98–S103	yes	22.0°N, 114.5°E	19.5°N, 117.0°E
I	1998.11.30–12.01	S087–S097	yes	23.0°N, 118.0°E	18.5°N, 119.5°E

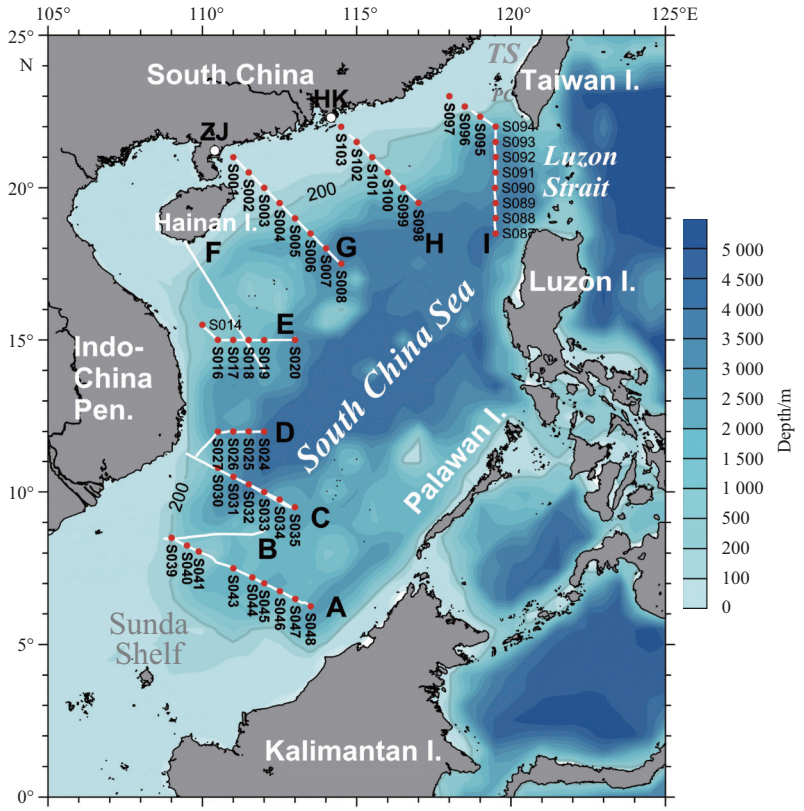

Fig. 1. Map of the SCS with CTD stations (red dots) and cross-shore sections of along-track ADCP measurements (white lines). HK represents Hong Kong, ZJ Zhanjiang, TS Taiwan Strait, and PC Penghu Channel.

der below the reported westward moving speeds of surface drifters surrounding the SCS perimeter (Centurioni et al., 2004, 2009), no tidal correction was applied to the ship-board ADCP current measurements. Nevertheless, the results over the inner portion of the continental shelf should be viewed with care, because tidal currents may not be negligible there. The ADCP data were decomposed into velocity components perpendicular and parallel to each section after quality control, which were than gridded for contouring and transport estimation. The cross-section transport was integrated from the gridded cross-section velocity and grid size for the southward flowing area of interest (see Section 3 and Table 2 for more details).

3 Structure of the SCSwwbc

Figures 2–4 present the observed distributions of temperature, salinity, density, and cross-sectional current velocity along all available sections. Analyses for Sections D, E and I are extended toward the coast with measurements along the corresponding broken track of the survey to obtain more details (Fig. 1).

The SCSwwbc was extremely strong off the coast of the ICP where ADCP measurements revealed a well-developed baroclinic jet along the western boundary (Fig. 2, right panels). The jet was swift and narrow, approximately 100 km in width and 400 m in depth; and it was surface-intensified with a core in the upper 200 m over the slope. The maximum cross-sectional currents for Sections A, C, D (Figs 2a, b and c) and B (Fig. 3a) were all greater than 160 cm/s. At the 400 m depth, the current velocity reduced to less than 10 cm/s, close to the level of uncertainty of the ADCP measurement.

The distributions of water properties off the ICP coast were generally consistent with the observed flow pattern (Fig. 2), where water in the core of the SCSwwbc was consistently warm-

Table 2. Cross-sectional transport estimates

Section	Observation date	Start		End		Transport[1)]/10^6 $m^3 \cdot s^{-1}$		
		North latitude	East longitude	North latitude	East longitude	Jet	Band	Net
A	1998.12.07 & 14	6.2°	113.5°	8.5°	109.0°	–15.5	–15.5	
B	1998.12.14–15	8.5°	108.8°	8.7°	112.0°	–19.9	–19.9	
C	1998.12.15–17	9.5°	113.0°	10.9°	109.6°	–18.7	–18.7	
D	1998.12.19–21	12.0°	109.8°	12.0°	112.0°	–22.3	–27.4	
E	1998.12.26	15.0°	110.0°	15.0°	113.0°	n/a	–23.7	
F	1998.12.21–23	18.2°	109.5°	14.0°	112.0°	–19.2	–30.3	
G	1998.12.27	21.0°	111.0°	17.5°	114.5°	–11.9	not found	–21.1
H	1998.11.28	22.0°	114.5°	19.5°	117.0°	not found	not found	+8.1
I	1998.11.30–12.01	23.0°	118.0°	22.0°	119.5°	not found	+11.9[(a)]	+4.3
	1998.12.01–12.02	22.0°	119.5°	18.5°	119.5°		–7.6[(b)]	

Note: [1)] Measurements in shelf areas shallower than 100 m are not included in the estimate. The currents along the extended ship courses of Sections D and E were decomposed in the same coordinates as the main leg. Band means the entire negative flowing water band near the coast except for Section I, for which estimates for the north (a) and the south (b) segments of the loop-like Kuroshio intrusion are given.

er, fresher and lighter than that further offshore. This pattern is clear at Section E (Fig. 2d), and can be found at other three sections (Figs 2a, b and c) although less obvious because of the short coverage range of the survey. The onshore pressure gradient produced by the density contrast obviously provided a main force that drove the southward flowing geostrophic current.

Offshore from the SCSwwbc, doming of the isolines is clearly visible along Sections A and C off the southeastern ICP, implying a cyclonic circulation around the dome (Fig. 2). Accompanied by the SCSwwbc, the northward recirculation manifested the subbasin scale "Nansha Gyre", a major feature of the southern SCS in winter (Fang et al., 2002), which is further evident from the strong northward flow at Section A to the east of the SCSwwbc (Fig. 2a, left panel). The strength and scales of the northward current were comparable with those of the SCSwwbc, indicating turning and re-circulation of the jet along the Sunda slope. Return flows (about 40 cm/s) can also be observed to the right of the jet at Sections B (Fig. 3a) and C (Fig. 2b), though less significant.

Farther north off the central ICP coast, a much wider band can be found flowing southward (approximately 150 km for Sections D and 200 km for Section E), whereas a well-shaped boundary jet with speeds greater than 160 cm/s was still there (Figs 2c and d). A similar pattern can also be seen at Section F where the southward flowing band (about 350 km) covered almost the entire section but the core speeds of the jet reduced to approximately 80 cm/s, about one-half of that to the south (Fig. 3b). It is thus suggested that in addition to the upstream jet, the SCSwwbc also entrained water from the interior SCS gaining strength on its way south.

A rather different situation was encountered in the northern SCS (Fig. 4). At Section G off Zhanjiang of South China, the SCSwwbc was barely observable hydrographically over the shelf break, and the maximal cross-sectional current reduced to about 40 cm/s (Fig. 4a). Nonetheless, a large volume of westward transport was still anticipated across the whole section, as currents were predominantly westward feeding the downstream SCSwwbc. This is also supported by the distributions of hydrographic properties in which doming of isotherm and isopycnal was found, suggesting southwestward geostrophic flow on the northwestern side of the dome, even though the shelf water was cooler and heavier than that further offshore (Fig. 4a).

Along Section H off Hong Kong, the SCSwwbc was no longer detectable from either water properties or current distributions, indicating that the SCSwwbc was confined to the west of Hong Kong (Fig. 4b). The property distributions showed a frequently observed trough at 20°N, (e.g., Li et al., 1998) suggesting a weak anticyclonic circulation off the slope that was possibly induced by intruded Kuroshio water (Nitani, 1972; Li and Wu, 1989; Farris and Wimbush, 1996). In contrast to Section G, the cross-sectional currents were weak and mostly eastward, while an anticyclonic structure was faintly visible around 20°N in agreement with the property distributions.

The existence of a Kuroshio-detached eddy or intruded loop became apparent at Section I (Fig. 4c), where the current distribution indicated a strong eastward jet-like structure flowing eastward along the continental slope with maximal speeds exceeding 120 cm/s and a wider band of westward flows farther south with maximum speeds over 80 cm/s. The temperature distribution also shows a pool of warm water near the slope with sharp fronts on both sides, manifesting a density structure consistent with the flow pattern.

Horizontally, the segment of the loop-like structure outgoing from the SCS was approximately 70 km in width centered at 22.1°N, and the core of the inflowing segment was of similar scale centered at approximately 21.5°N (Fig. 4c, right panel). Hence, its overall scale was about 150 km, which is in good agreement with previous investigations (Li and Wu, 1989; Li et al., 1998). Vertically, the pattern extended from the surface to the range of our current measurement, suggesting that its vertical scale was greater than 400 m.

The most important fact revealed by the above observations is that there was not direct connection between the baroclinic SCSwwbc and the Kuroshio at the time of the survey. The SCSwwbc is most likely mainly a component of the interior recirculation of the SCS, but not a "branch" of the Kuroshio from the LS, at least not in December 1998.

4 Estimates of volume transport

Cross-sectional transports in the upper 400 m were estimated for all available ADCP sections, assuming that the surface current was identical to the first bin of the measurement (Fig. 1, Table 2). Three different types of transport estimate are given in the table: that of the narrow western boundary jet ("jet"), defined as the well shaped part of the flow field (about 100 km in width); the entire southward flowing band ("band"), which was much wider than the jet in some cases; and the net transport across the entire section ("net"), which is given for Sections G, H and I only.

Depending on the strength and pattern of the local circulation, and on the orientation of a section, the estimated "jet" transport ranges from -11.9×10^6 m^3/s to -22.3×10^6 m^3/s in the

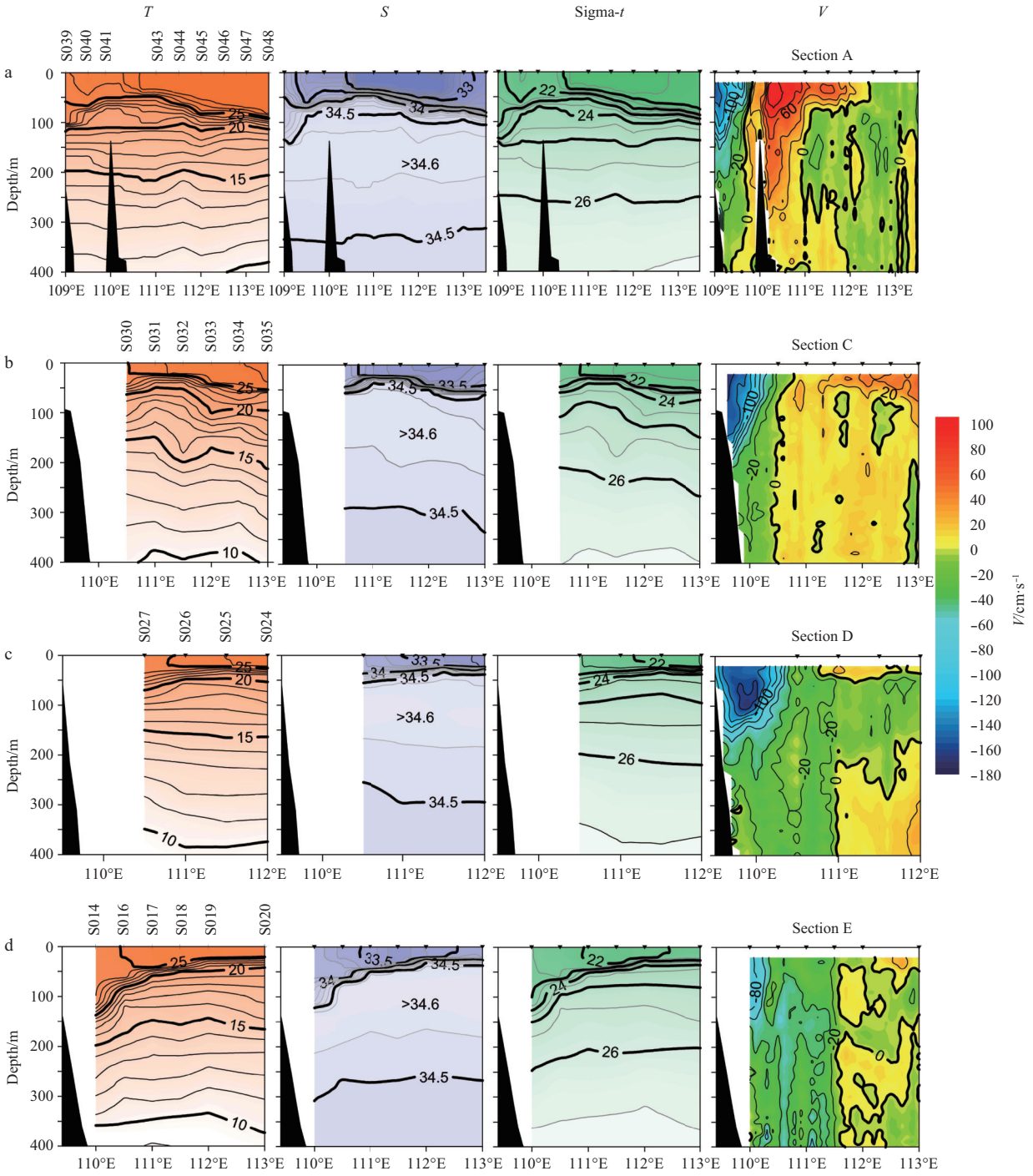

Fig. 2. Temperature (°C), salinity, sigma-*t*, and cross-sectional current (cm/s) along Sections A (a), C (b), D (c), and E (d), showing the southward (negative) flowing SCSwwbc. Note that east-west direction was taken as the orientation of Sections D and E when computing cross-sectional currents, even though they were extended toward the coast with changed ship courses.

western boundary area (negative value for southward transport). The jet was most robust off the ICP coast (form Sections F to B) where its transport was about –20×10^6 m^3/s with a maximum of –22.3×10^6 m^3/s found at Section D.

The estimated "jet" transport decreased either up or down the stream from the ICP coast. It reduced to –15.5×10^6 m^3/s at Section A down the stream. At Section G up the stream, the "jet" transport was –11.9×10^6 m^3/s only, yet the cross-sectional currents were westward generally (Fig. 4a), leading to a "net" transport of –21.1×10^6 m^3/s. It is thus evident that about one-half of the downstream transport of the SCSwwbc off the ICP was fed by the recirculation from the interior of the SCS other than the upstream jet.

The most significant fact revealed by these analyses is that the "net" transport to the east of the Zhujiang (Pearl) River Mouth was in the opposite direction of the SCSwwbc; the two transports were +8.1×10^6 m^3/s and +4.3×10^6 m^3/s (northeastward) across Section H off Hong Kong and across Section I in the LS (Table 2), respectively. This leads to the question that whether or not the Kuroshio is the main source the SCSwwbc as indicated by sur-

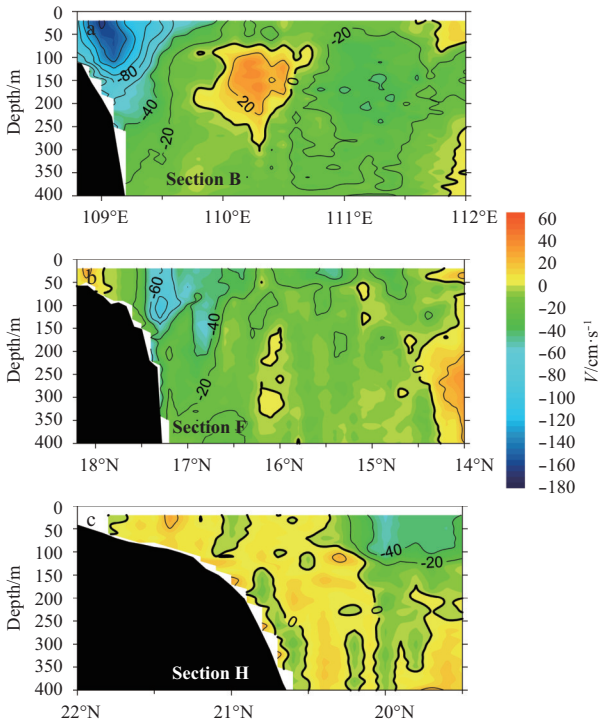

Fig. 3. Distributions of cross-sectional current (cm/s, negative for southward) along Sections B (a) and F (b), and along-sectional current (positive for offshore) along Section H (c).

face drifter measurements (Li et al., 2000; Centurioni et al., 2004; Qiu et al., 2011). The positive transport implies that during the survey, the SCSwwbc drew water mainly from the interior SCS rather than from the LS. In fact, onshore (negative) currents in the order of 40 cm/s were clearly presented at Section H in the upper 150 m off the slope (Fig. 3c), indicating interior feeding from the south. This onshore flow was also evident in the altimetry analysis of Wu et al. (2002) for the period of the survey.

The positive net transport across Section I was a result of the loop-like structure of the Kuroshio intrusion (Fig. 4c), for which the estimated "jet" transports of the well-shaped incoming and outgoing segments of the loop were -7.6×10^6 m^3/s and $+11.9\times10^6$ m^3/s, respectively, leaving a difference of $+4.3\times10^6$ m^3/s eastward (Table 2). Since the net cross-sectional transport through the section was positive and the transport to the south of 21°N was small, it is likely that the water in the SCS was entrained by the loop-like structure, leading to an increase of outgoing transport across the section. It seems that part of this outgoing transport eventually entered the Taiwan Strait through the Penghu Channel, where currents are generally northward year round (Chuang, 1986).

5 Discussion

Several important aspects about the strong SCSwwbc were revealed in full scale by the survey conducted in December 1998. The current flowed along the shelf edge all the way from the northern SCS to the west of Hong Kong down to the Sunda Shelf, where it turned cyclonically following the topography and departed from the western boundary. The current appeared baroclinic with a width around 100 km and a vertical scale of about 400 m.

The SCSwwbc was the most prominent feature of the SCS winter circulation during the survey. It was most energetic along the ICP coast where the maximum speed at the core of the current was greater than 160 cm/s. Upstream from there in the northern SCS to the west of Hong Kong, the current appeared weak and poorly organized, though traceable.

The SCSwwbc was not observed to the east of Hong Kong during the survey. Instead, an anticyclonic Kuroshio intrusion was found near the LS, which implies that a large portion of the Kuroshio water that entered the SCS looped back and returned to the Pacific. This result differs from what observed by surface drifting buoys, which generally pursue their journeys westward along the continental margin (Li et al., 2000; Centurioni et al., 2004, 2009). It is thus suggested that the main water body below the mixed layer behaves differently from the surface, and that the Kuroshio is not the main water source of the SCSwwbc. The SCSwwbc is most likely drawing water mainly from the interior recirculation rather than from the Kuroshio except in the near surface layer where the Ekman transport driven by the northeast monsoon may dominate.

On the basis of model results, Su and Liu (1992) suggested that the upstream source of the westward flowing current along the northern slope of the SCS in winter may not originate from the branching Kuroshio in the LS, but from the northward recirculation on the eastern side of the SCS. This is now supported by our observations. The recirculation may come mainly from the Luzon Gyre—a large-scale cyclonic circulation in the northern SCS (Fang et al., 1998; Li et al., 2003; Zheng et al., 2006), which appears in fall and lasts to late spring (e.g., Li et al., 2000). Therefore, the SCSwwbc is most likely the western boundary current of the basin-scale wind-driven circulation of the SCS proper, which is only partially sustained by the surface transport through the LS.

As a corollary, the Pacific-to-Indian Ocean interbasin flow through the SCS, known as the SCS Throughflow (e.g., Lebedev and Yaremchuk, 2000; Fang et al., 2005; Qu et al., 2005), is likely not a persistent, well-organized ocean current in the normal sense, but a bulk transport from the Pacific to the Indonesian seas through the SCS. Even though the SCSwwbc may contribute to the transport of the SCS Throughflow, they are different in concept. The transport out of the Kerimata Strait (a mean of approximately 1×10^6 m^3/s with a winter maximum of approximately 4×10^6 m^3/s, according to Fang et al. (2009)) is far smaller than that of the SCSwwbc (approximately 20×10^6 m^3/s from our observation).

It is likely that the interbasin transport through the LS in winter, when the northeasterly wind prevails, can be attributed mainly to wind-forced Ekman drift in the LS (Wyrtki, 1961), which flows westward generally as revealed by the movement of surface drifters (Centurioni et al., 2004). The drifters that enter the LS were then carried westward by the drift falling into the SCSwwbc regime and continuing their journey to the west. In other wards, the Ekman drift builds a bridge in the near-surface layer that links the SCSwwbc to the Kuroshio, providing a pathway for the SCS Throughflow.

Furthermore, while advecting cold water to the south near the surface and causing a "gap" of the Indo-Pacific warm pool in the boreal winter (Liu et al., 2004), the subsurface water of the SCSwwbc is actually warmer, fresher, and hence lighter than the interior of the basin. That provides a cross-shore, baroclinic driving force for the SCSwwbc, although the cross-shore barotropic pressure gradient set up by the northeast monsoon may also play a role.

Finally, previous studies reported significant interannual variation in the general circulation of the SCS associated with ENSO events (Fang et al., 2006; Xing et al., 2012; Wu and Chang, 2005),

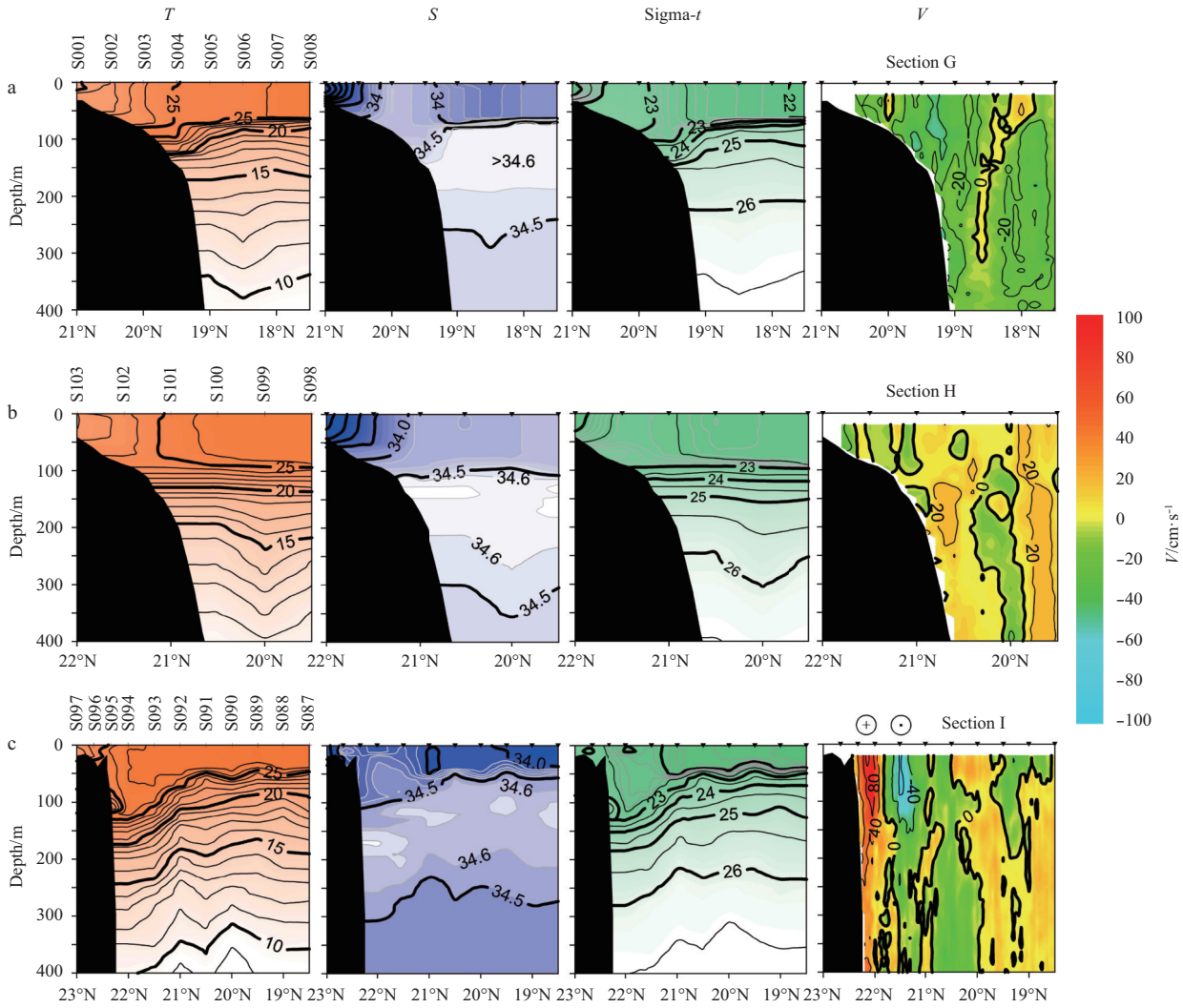

Fig. 4. Same as Fig. 2, except for Section G, where currents were generally negative (southwestward) and the SCSwwbc over the slope was weak (a); for Section H, where currents were mainly positive (b); and for Section I, where a loop-like Kuroshio intrusion or detached eddy was clearly present off the slope (c).

and an anomalous strong cyclonic circulation of the SCS in the winter of 1998/1999 in a global model (Wang et al., 2006). It has also been shown through observations that from 1992 to 2014, the maximal winter transport of the SCSwwbc across a section off the southeastern shelf break of the Hainan Island was 11.8×10^6 m^3/s southward, with a range of fluctuation of the yearly southward maximum of about 5×10^6 m^3/s (Zhu et al., 2015). Hence, the SCSwwbc may also subject to interannual variation related to the ENSO (Quan et al., 2016). A question left to consider is whether the observed strong transport in the winter of 1998 is a climatologically normal state, or a special case.

It is known that the ENSO generally weakens the circulation of the SCS and decelerates its western boundary current during the late winter of an El Niño year (Chao et al., 1996; Liu et al., 2004). Since our observation was conducted one year after the peak phase of the 1997/1998 ENSO when a moderate La Niña was developing, the results of this study may reflect the situation of a somehow stronger SCSwwbc than that of a normal year. However, according to the result of Zhu et al. (2015), the transport of the SCSwwbc off the Hainan Island was not significantly different in December 1998 from most other years. Further study is needed to resolve the interannual variation of the SCSwwbc.

6 Conclusions

For the first time, a full 3-D image of the SCSwwbc is presented by using direct current measurements. On the basis of the results of the survey, the following conclusions are evident. (1) The SCSwwbc emerged off the shelf edge off Hong Kong and was confined to the west of that location, which flowed all the way from the Hainan Island to the Sunda Shelf along the continental margin. The current was about 1 700 km in length, 100 km in width, and 400 m in depth. (2) The SCSwwbc appeared to be the most distinct feature of the basin-wide winter circulation of the SCS. It was the strongest off the ICP coast, where its volume transport reached over 20×10^6 m^3/s, a strength comparable with the major western boundary currents. (3) In the period of our observations, the SCSwwbc was fed primarily by the interior recirculation of the SCS.

Our observational results also suggest that: (1) the interbasinal SCS Throughflow likely contributes only a minor portion to the total transport of the SCSwwbc; and (2) in the western boundary area, the subsurface water of the SCSwwbc was warmer, fresher, and lighter than the interior water of the SCS basin, which provided a baroclinic driving force for the SCSwwbc. Further investigation is necessary to verify these findings.

Acknowledgements

The field survey was supported by the State Oceanic Administration. We appreciate the assistance and enthusiasm of the crew of R/V *Xiangyanghong 14* and the scientific party onboard.

References

Centurioni L R, Niiler P P, Lee D K. 2004. Observations of inflow of Philippine Sea surface water into the South China Sea through the Luzon Strait. Journal of Physical Oceanography, 34(1): 113–121

Centurioni L R, Niiler P N, Lee D K. 2009. Near-surface circulation in the South China Sea during the winter monsoon. Geophysical Research Letters, 36(6): L06605, doi: 10.1029/2008GL037076

Chao S Y, Shaw P T, Wu S Y. 1996. El Niño modulation of the South China Sea circulation. Progress in Oceanography, 38(1): 51–93

Chuang W S. 1986. A note on the driving mechanisms of current in the Taiwan Strait. Journal of Oceanography, 42(5): 355–361

Dong Huichao, Jing Zhiyou, Qi Yiquan, et al. 2013. Dynamic analysis on the winter current over western boundary of the South China Sea. Journal of Tropical Oceanography (in Chinese), 32(2): 74–81, doi: 10.11978/j.issn.1009-5470.2013.02.008

Fang Guohong, Fang Wendong, Fang Yue, et al. 1998. A survey of studies on the south china sea upper ocean circulation. Acta Oceanographica Taiwanica, 37(1): 1–16

Fang Wendong, Fang Guohong, Shi Ping, et al. 2002. Seasonal structures of upper layer circulation in the southern South China Sea from in situ observations. Journal of Geophysical Research: Ocean, 107(C11): 3202, doi: 10.1029/2002JC001343

Fang Wendong, Guo Junjian, Shi Ping, et al. 2006. Low frequency variability of South China Sea surface circulation from 11 years of satellite altimeter data. Geophysical Research Letters, 33(22): L22612, doi: 10.1029/2006GL027431

Fang Guohong, Susanto D, Soesilo I, et al. 2005. A note on the South China Sea shallow interocean circulation. Advances in Atmospheric Sciences, 22(6): 946–954

Fang Guohong, Wang Gang, Fang Yue, et al. 2012. A review on the South China Sea western boundary current. Acta Oceanologica Sinica, 31(5): 1–10

Fang Guohong, Wang Yonggang, Wei Zexun, et al. 2009. Interocean circulation and heat and freshwater budgets of the South China Sea based on a numerical model. Dynamics of Atmospheres and Oceans, 47(1-3): 55–72

Farris A, Wimbush M. 1996. Wind-induced Kuroshio intrusion into the South China Sea. Journal of Oceanography, 52(6): 771–784

He Zhigang, Wang Dongxiao. 2009. Surface pattern of the South China Sea western boundary current in winter. In: Gan Jianping, ed. Advances in Geosciences, Volume 12: Ocean Science. Singapore: World Scientific Publishing Company, 99–107, doi: 10.1142/9789812836168_0008

Lebedev K V, Yaremchuk M I. 2000. A diagnostic study of the Indonesian Throughflow. Journal of Geophysical Research: Ocean, 105(C5): 11243–11258, doi: 10.1029/2000JC900015

Li Li. 2008. Upper layer circulation in the South China Sea. In: Liu A K, Ho C R, Liu C T, eds. Satellite Remote Sensing of South China Sea. Taipei: Tingmao Publish Co, 275–290

Li Li, Nowlin W D Jr, Su Jilan. 1998. Anticyclonic rings from the Kuroshio in the South China Sea. Deep-Sea Research: Part I. Oceanographic Research Papers, 45(9): 1469–1482

Li Li, Wu Boyu. 1989. A Kuroshio loop in South China Sea?—On circulations of the northeastern South China Sea Journal of Oceanography in Taiwan Strait (in Chinese), 8(1): 89–95

Li Li, Wu Risheng, Guo Xiaogang. 2000. Seasonal circulation in the South China Sea—A TOPEX/Poseidon satellite altimetry study. Haiyang Xuebao (in Chinese), 22(6): 13–26

Li Li, Xu Jindian, Jing Chunsheng, et al. 2003. Annual variation of sea surface height, dynamic topography and circulation in the South China Sea: a TOPEX/Poseidon satellite altimetry study. Science in China: Series D. Earth Sciences, 46(2): 127–138

Liu Qinyu, Jiang Xia, Xie S P, et al. 2004. A gap in the Indo-Pacific warm pool over the South China Sea in boreal winter: seasonal development and interannual variability. Journal of Geophysical Research: Ocean, 109(C7): C07012, doi: 10.1029/2003JC002179

Lyu Kewei, Yang Xiaoyi, Zheng Quanan, et al. 2016. Intraseasonal variability of the winter western boundary current in the South China Sea using satellite data and mooring observations. IEEE Journal of Selected Topics in Applied Earth Observations and Remote Sensing, 9(11): 5079–5088, doi: 10.1109/JSTARS.2016.2553049

Nitani H. 1972. Beginning of the Kuroshio. In: Stommel H, Yoshida K, eds. Kuroshio: Physical Aspects of the Japan Current. Tokyo: University of Washington Press, 129–163

Qiu Yun, Li Li, Chen C T A, et al. 2011. Currents in the Taiwan Strait as observed by surface drifters. Journal of Oceanography, 67(4): 395–404, doi: 10.1007/s10872-011-0033-4

Qu Tangdong, Du Yan, Meyers G, et al. 2005. Connecting the tropical Pacific with Indian Ocean through South China Sea. Geophysical Research Letters, 32(24): L24609, doi: 10.1029/2005GL024698

Quan Qi, Xue Huijie, Qin Huiling, et al. 2016. Features and variability of the South China Sea western boundary current from 1992 to 2011. Ocean Dynamics, 66(6 - 7): 795–810, doi: 10.1007/s10236-016-0951-1

Su Jilan, Liu Xianbing. 1992. The circulation simulation of the South China Sea. In: Zeng Qingcun, Yuan Chongguang, Zhao Jianping, et al., eds. Collected Papers of the Symposium on Ocean Circulation (in Chinese). Beijing: China Ocean Press, 206–215

Tian Yongqing, Pan Aijun, Zeng Mingzhang. 2015. A study on the temporal and spatial characteristics of the South China Sea western boundary current and its relationship with ENSO cycle. Journal of Applied Oceanography (in Chinese), 34(1): 1–9, doi: 10.3969/J.ISSN.2095-4972.2015.01.001

Wang Yonggang, Fang Guohang, Wei Zexun, et al. 2006. Interannual variation of the South China Sea circulation and its relation to El Niño, as seen from a variable grid global ocean model. Journal of Geophysical Research: Oceans, 111(C11): C11S14, doi: 10.1029/2005JC003269

Wang Dongxiao, Liu Qinyan, Xie Qiang, et al. 2013. Progress of regional oceanography study associated with western boundary current in the South China Sea. Chinese Science Bulletin, 58(11): 1205–1215, doi: 10.1007/s11434-012-5663-4

Wu C R, Chang C W J. 2005. Interannual variability of the South China Sea in a data assimilation model. Geophysical Research Letters, 32(17): L17611, doi: 10.1029/2005GL023798

Wu Risheng, Guo Xiaogang, Li Li. 2002. Winter hydrographic condition and circulation of the South China Sea in 1998. Haiyang Xuebao (in Chinese), 24(S1): 142–153

Wyrtki K. 1961. Physical oceanography of the Southeast Asian waters. NAGA Report, Vol. 2. Scientific Results of Marine Investigations of the South China Sea and the Gulf of Thailand 1959–1961. San Diego: Scripps Institute of Oceanography, 1–195

Xing Yansong, Cheng Guosheng, Shu Yeqiang, et al. 2012. Anomalous characteristics of the ocean circulation in South China Sea during the El Niño events. Oceanologia et Limnologia Sinica (in Chinese), 43(2): 201–209

Zhang Zhixin, Guo Jingsong, Guo Binghuo. 2016. Reversal process of the South China Sea western boundary current in autumn 2011. Chinese Journal of Oceanology and Limnology, 34(3): 608–618, doi: 10.1007/s00343-016-4388-7

Zheng Quanan, Fang Guohong, Song Y T. 2006. Introduction to special section: dynamics and circulation of the Yellow, East, and South China Seas. Journal of Geophysical Research: Oceans, 111(C11): C11S01, doi: 10.1029/2005JC003261

Zhu Xiaohua, Zhao Ruixiang, Guo Xinyu, et al. 2015. A long-term volume transport time series estimated by combining in situ observation and satellite altimeter data in the northern South China Sea. Journal of Oceanography, 71(6): 663–673, doi: 10.1007/s10872-015-0305-5

Zu Tingting, Gan Jianping, Erofeeva S Y. 2008. Numerical study of the tide and tidal dynamics in the South China Sea. Deep Sea Research: Part I. Oceanographic Research Papers, 55(2): 137–154, doi: 10.1016/j.dsr.2007.10.007